AMERICAN SCIENTIFIC PUBLISHERS

Science of Advanced Materials
Vol. 5, pp. 1686–1693, 2013
(www.aspbs.com/sam)

ARTICLE

Synthesizing the Composites of Graphene Oxide-Wrapped Polyaniline Hollow Microspheres for High-Performance Supercapacitors

Mancheng Liu[1], Xilin Wu[1,2], Changlun Chen[1,*], Qi Wang[1], Tao Wen[1], and Xiangke Wang[1,*]

[1]*Key Laboratory of Novel Thin Film Solar Cells, Institute of Plasma Physics, CAS, 230031, Hefei, China*
[2]*College of Nuclear Science and Technology, University of Science and Technology of China, 230000, Hefei, China*

ABSTRACT

The novel composites of graphene oxide-wrapped polyaniline (PGO) hollow microsphere have been synthesized through a facile self-assembly method. Driven by the mutual electrostatic interactions, the polyaniline (PANI) hollow microspheres prepared by a simple copper(II)-catalyzed process are fully wrapped by graphene oxide (GO) sheets. The composites with various weight feed ratios of PANI to GO sheets are also fabricated and characterized by different methods. The electrochemical tests show that the electrochemical performances of PGO composites depend largely on the mass ratios of PANI to GO sheets. Compared with the electrode materials of PANI and other PGO composites, the PGO20 composite has the highest specific capacitance of 731.2 F/g at a scan rate of 5 mV/s and good charge/discharge cycling stability (95% of the preserved capacitance is conserved after 2000 cycles). The substantially improved electrochemical performances of PGO composites are ascribed to the synergistic effects between the conductive PANI hollow microspheres and the GO sheets. The excellent electrochemical performance suggests promising application of PGO composites in high-performance supercapacitors.

KEYWORDS: Graphene Oxide, Polyaniline, Supercapacitors.

1. INTRODUCTION

With the depleting of traditional energy resource and increasing pollution, the development of rechargeable high power energy storage devices has been attracted much attention in recent years.[1] Electrochemical supercapacitors are possible candidates for the high power energy storage systems due to their longer cycle life and power density compared to lithium-ion batteries[2,3] and higher energy density than conventional dielectric capacitors. In particular, supercapacitors made up of conducting polymers show superior capacitance performance resulting from the fast and reversible redox processes related to the π-conjugated polymer chains.[4]

Among these conducting polymers, polyaniline (PANI) is considered as the most promising material for its low cost, facile synthesis,[5,6] higher capacitance,[7,8] and adjustable electrical conductivity by oxidation or protonation.[9,10] PANI hollow spheres have drawn considerable interest recently due to their unique properties, such as low density, high specific surface area, and good permeation. PANI hollow spheres also demonstrated good electrical conductivity[11] and excellent electrochemical properties.[12] However, the relative poor cycling life limits its widespread application.[13] To make up for the defect, the composites of PANI hollow spheres complexed with other materials, such as polystyrene,[14] MnO_2[15] and carbon nanotubes,[16] have been widely studied because of their outstanding thermal, mechanical and electrochemical properties.

Different from the mentioned materials, graphene or graphene oxide (GO) that obtained from graphite by a variety of methods,[17–19] possesses large surface area, moderate conductivity, good chemical stability and mechanical property. Unfortunately, graphene that don't have hydrophilic radicals inevitably causes aggregation of graphene nanosheets, and extremely easily separates with other materials. To solve this problem, GO (the modified graphene by chemical modifications or non-covalent functionalizes) is the most easily synthesized and dispersed graphene derivative, which has been widely used in material chemistry and basic research.[20,21] For instance, Liu[22] reported a novel and facile synthesis of a high quality GO-PANI composite by *in situ* polymerization suitable for supercapacitor application. To our best knowledge, there is

*Authors to whom correspondence should be addressed.
Emails: clchen@ipp.ac.cn, xkwang@ipp.ac.cn
Received: 12 December 2012
Accepted: 21 May 2013

no report on graphene oxide-wrapped polyaniline (PGO) hollow microspheres by mutual electrostatic interactions between positively charged PANI hollow microspheres and GO sheets. Therefore, the unique properties of GO sheets mentioned above promised us to synthesize the composites for high-performance supercapacitors.

In this paper, we reported the novel composites of PGO hollow microspheres by mutual electrostatic interactions between positively charged PANI hollow microspheres and GO sheets. And we also studied the influence of the mass ratios on the morphologies of the composites, and further studied the impact on the electrochemical performance.

2. EXPERIMENTAL DETAILS

2.1. Synthesis of GO

GO was prepared from natural graphite (crystalline, 300 mesh, 99.95% purity, Qingdao Tianhe Graphite Co. Ltd., China) by a modified Hummers method.[23] In a typical method, Graphite (3 g) and $NaNO_3$ (2.25 g) were mixed with 225 ml of H_2SO_4 (98%) in a 1000 ml flask. The mixture was stirred for 30 min within an ice bath. While maintaining vigorous stirring, $KMnO_4$ (13.5 g) was gradually added to the solution. The adding rate was carefully controlled to keep the reaction temperature below 20 °C. The ice bath was then removed, and the mixture was stirred at room temperature for 5 d. Subsequently, the reaction mixture was slowly diluted with 420 ml Milli-Q water where the temperature rapidly increased to 98 °C. After the temperature was reduced to 60 °C, 9 ml H_2O_2 (30%) was added to the mixture. The resulting suspension was ultrasonicated for 1 h and vigorously stirred overnight. The solid was obtained from centrifugation (19000 rpm, 20 min) followed by washing with excess Milli-Q water for several times until the solution was neutral. The product was dried in a vacuum tank at room temperature for 12 h and the desired GO was obtained.

2.2. Synthesis of PANI Hollow Microspheres

The PANI hollow microspheres were synthesized by a one step copper(II)-catalyzed self-assembly method.[24] Typically, 6 mmol aniline was first dispersed in 20 ml Milli-Q water under magnetic agitation at room temperature for 15 min. The aniline solution was then cooled in an ice-water bath for 3 min. Afterwards, an aqueous solution containing 0.75 mmol copper chloride dehydrate and 6 mmol ammonium persulfate, precooled in the ice-water bath for 3 min, was added to the aniline solution, and the reaction was carried out in the ice-water bath without magnetic stirring. After 12 h, the resulting dark green PANI was obtained followed by centrifugation and rinsed with Milli-Q water and ethanol for several times. Then the product was dried in an oven for 24 h at 60 °C.

2.3. Synthesis of PGO Composites

PGO composites were synthesized via electrostatic interaction between PANI and GO by mixing their correspondingly aqueous solutions together with vigorous stirring under the ambient environment. The mass ratios of PANI to GO were varied as 90:10, 80:20, 50:50, and 20:80, and the resulting composites were named as PGO10, PGO20, PGO50, and PGO80, respectively. The samples of PGO30 and PGO40 were also prepared and their electrochemical properties were measured and we found that their special capacitances declined after the PGO20. PGO50 was selected as the typical intermediate point between PGO20 and PGO80. The synthesis processes were schematically shown in Scheme 1(a). Firstly, PANI and GO were dispersed in Milli-Q water by bath-sonicating for 20 min, respectively. Then the two aqueous solutions were mixed together and magnetically stirred at room temperature overnight. The product was collected by centrifugation and washed with deionized water for several times. The final PGO composites were dried in a vacuum oven at room temperature for 12 h.

2.4. Characterization

Field emission scanning electron microscopic (FE-SEM) images of the samples were obtained from a JEOL JSM-6330F. Transmission electron microscopic (TEM) were performed on a JEOL-2010 microscope. The powder X-ray diffraction (XRD) patterns were measured on a (Philips X'Pert Pro Super X-ray) diffractometer with a Cu Ka source ($\lambda = 1.541$ Å). Fourier transformed infrared spectra (FT-IR) spectroscopy measurements were mounted by using a Perkin-Elmer 100 spectrometer over a range from 500 to 4000 cm^{-1}. The X-ray photoelectron spectroscopy (XPS) measurements were conducted with a VG Scientific ESCALAB Mark II system. The specific surface areas were determined by nitrogen adsorption–desorption isotherms (Tristar II 3020 M, Micromeritics Co., USA).

2.5. Electrochemical Measurement

The working electrodes were prepared by mixing the as-prepared composites and polytetrafluoroethylene (from 60 wt.% water suspension, Aldrich) with the mass ratio 95:5 in ethanol. Then, the mixture was dropped onto glassy carbon electrode with a diameter of 5 mm for 2 h at 50 °C to remove the solvent. The supercapacitor devices are fabricated in Scheme 1(b). And all electrochemical measurements were carried out on a CHI660D electrochemical workstation in 2 M H_2SO_4 by using a three electrode system, in which platinum foil and Ag/AgCl electrode filled with 3 M KCl were used as counter and reference electrode. Cyclic voltammetry (CV) and galvanostatic charge/discharge tests were performed at the voltage window of −0.2–0.80 V, and electrochemical impedance spectroscopy (EIS) measurements were also conducted in the

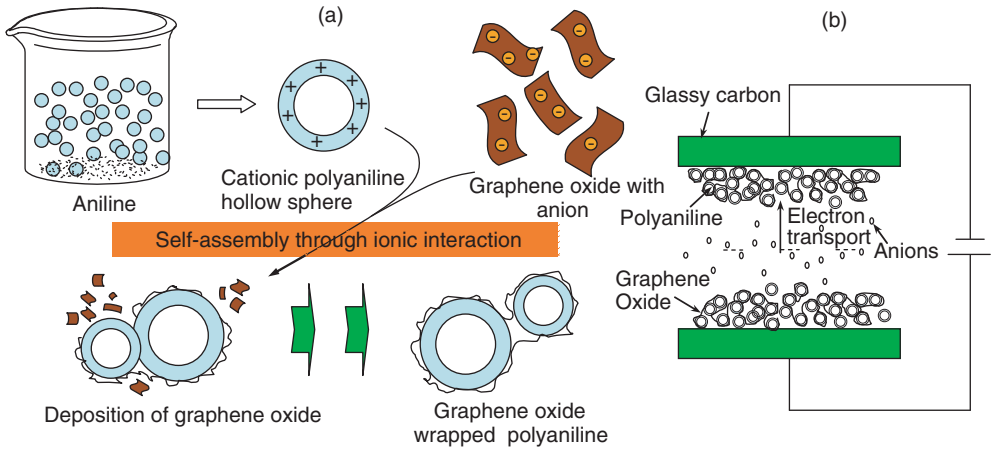

Scheme 1. Schematic illustration of the synthesis of PGO hollow microspheres (a), and the diagram of PGO supercapacitor device (b).

frequency range of 100 kHz–0.01 Hz at room temperature. For this three-electrode system, the specific capacitance of the active electrode materials was determined by the cyclic voltammetry curves or the galvanostatic charge/discharge curves:

$$C = \frac{\int i dt}{m\Delta V} \quad (1)$$

$$C = \frac{I\Delta t}{m\Delta V} \quad (2)$$

where C is the specific capacitance, i is the oxidation or reduction current, dt is time differential, m is the mass of active material, V is the potential window, I is charge or discharge current, and t is the time for a full charge or discharge.

3. RESULTS AND DISCUSSION

3.1. Characterization of PGO Composites

The morphologies of PANI and PGO composites were studied by SEM and TEM images. The as-synthesized PANI hollow microspheres are fairly uniform in size (Fig. 1(a)) and the shell thickness is approximately 100 nm (Fig. 1(d)). From the inset of Figure 1(a), the microsphere has a hole on the surface, indicating that the microspheres are hollow. In the PGO20 composite (Figs. 1(b) and (c)), the GO nanosheets wrapped the PANI hollow microspheres completely have only several thin-layers and some wrinkles on the surfaces. As GO contents in PGO composites change, the GO nanosheets wrap the microspheres partially (Fig. 2(a)) or overly (Fig. 2(b)). And GO sheets agglomerate together and are separated from the PANI microspheres in the PGO80 composite (Fig. 2(c)).

Figure 3(a) shows the XRD patterns of GO, PANI and PGO composites. The broad diffraction peak at $2\theta = 10.8°$ ($d \approx 0.85$ nm), which corresponds to the typical diffraction peak of GO sheets, is attributed to the (002) plane. And the PANI hollow microspheres have two broad peaks at approximately $2\theta = 21°$ and 25°. The peak located at $2\theta = 21°$ is due to the periodicity parallel to the PANI chains, while the $2\theta = 25°$ peak is ascribed to the periodicity perpendicular to the PANI chains.[25] With the increase of the GO mass ratios in the composites, the diffraction peaks of GO are enhanced and those of PANI are weakened gradually.

Figure 3(b) shows the FT-IR spectra of GO, PANI, and PGO20 composite. The characteristic peaks at 1728, 1631, 1411, and 1062 cm^{-1} in the GO spectrum are attributed to the C═O in COOH, intercalated water, the CO—H groups, and the C—O in C—O—C functional groups, respectively, which are consistent with the previous reports.[26] And for the PANI sample, the absorption peaks centered at 1590 and 1501 cm^{-1} are ascribed to the C═C stretching vibration of the quinoid ring and benzenoid rings in the emeraldine salt.[27] Simultaneously, the peaks at 1306, 1143, and 827 cm^{-1} are corresponding to the C—N stretching of the secondary aromatic amine, the C═N stretching, and the aromatic C—H bending,

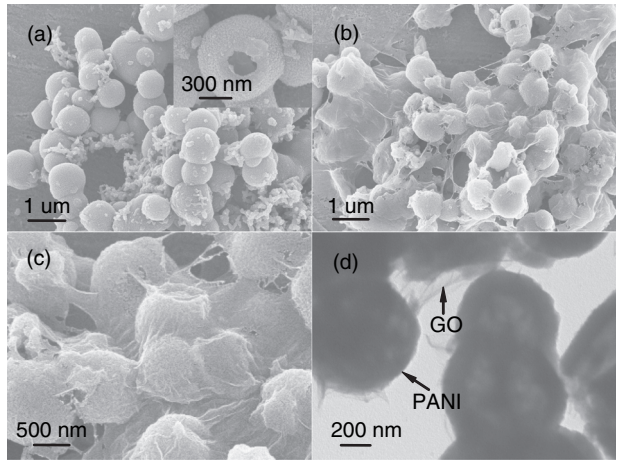

Fig. 1. SEM images of PANI (a), the inset is FE-SEM image of PANI. PGO20 (b), FE-SEM image of PGO20 (c), and TEM image of PGO20 (d).

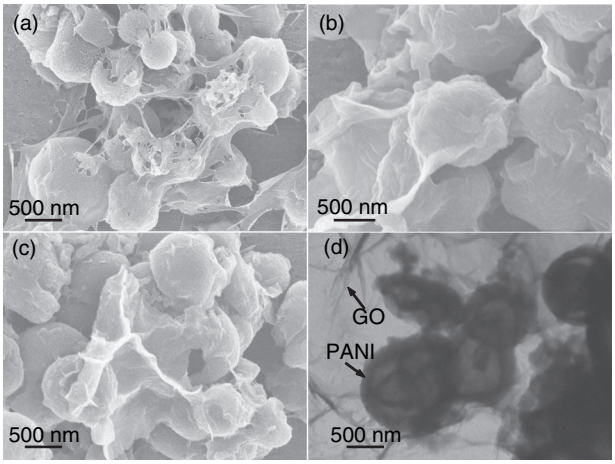

Fig. 2. SEM images of PGO10 (a), PGO50 (b) and PGO80 (c), TEM images of PGO80 (d).

respectively. By comparison, the spectrum of the PGO20 composite has the peaks of both GO and PANI with the peaks of C═O and O—H groups from GO and strong peaks of functional groups from PANI.

The composition of as-prepared composites can be provided by XPS. The XPS wide spectrum (Fig. 3(c)) of PGO20 shows that the C1s binding energy is approximately 285 eV, and those of N1s and O1s are approximately 400 and 532 eV, respectively. The C1s core-level spectrum shown in Figure 3(d) can be curve-fitted into six peak components with binding energies at about 284.4, 284.7, 285.2, 286.9, 287.8, and 289.1 eV, attributed to C—C, C═C, C—N, C—O, C═O, and O—C═O species, respectively.[28] The spectrum of C1s observed at 285 eV for GO is slightly decreased to 284.4 eV after the GO wrapped on the PANI microspheres. This result is probably attributed to the decrease in the conjugation as well as in the hydrogen bonds of the GO sheets and the PANI microsphere surface. Besides, the C1s of O—C═O peak increases to 289.1 eV, indicating that the COOH groups of GO were linked to the PANI microsphere surface by electrostatic interaction.

3.2. Electrochemical Performance of PGO Composites

The electrochemical performance of PGO composites used as electrode materials for supercapacitors is evaluated by standard CV and galvanostatic charge/discharge technique in 2 M H_2SO_4. It can be seen from Figure 4(a) that the GO electrode shows a very featureless current response in the CV curve and its specific capacitance is less than 5 F/g probably due to the low electrical conductivity of GO. The CV curve of the GO shown in Figure 4(b) is nearly rectangular in shape and shows one pair of redox peaks due to the transition between quinone/hydroquinone states, which is typical for carbon materials with oxygen-containing

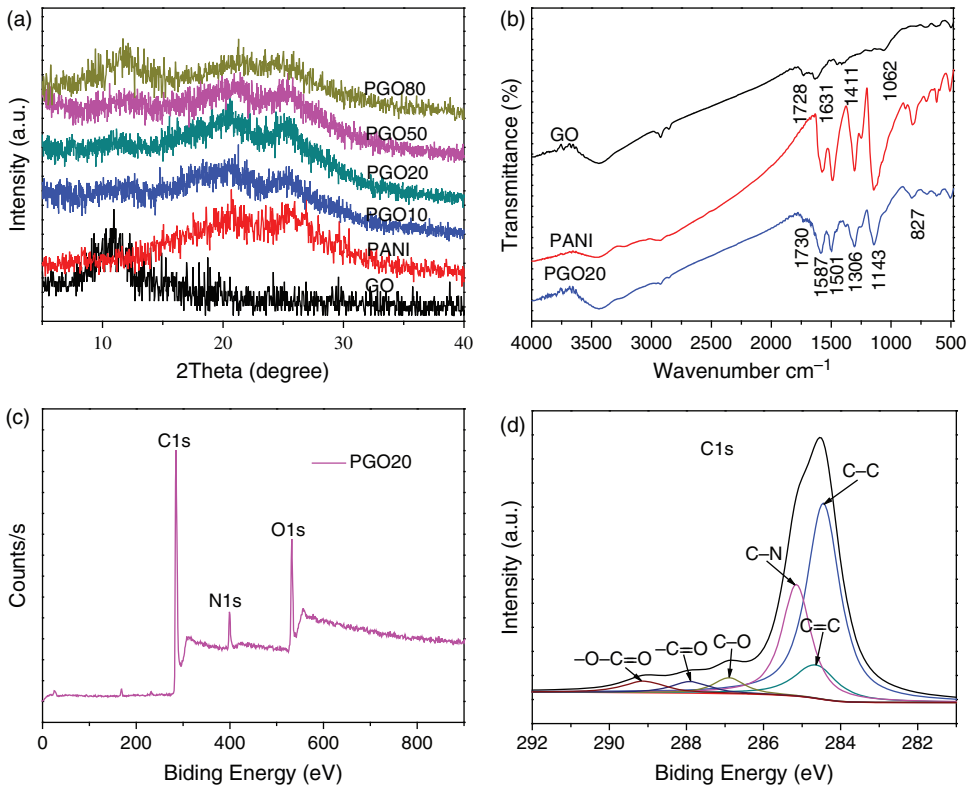

Fig. 3. XRD patterns of GO, PANI and PGO composites (a), FT-IR spectra of GO, PANI and PGO20 (b), XPS spectrum of PGO20 (c), and XPS C 1s core-level spectra of PGO20 (d).

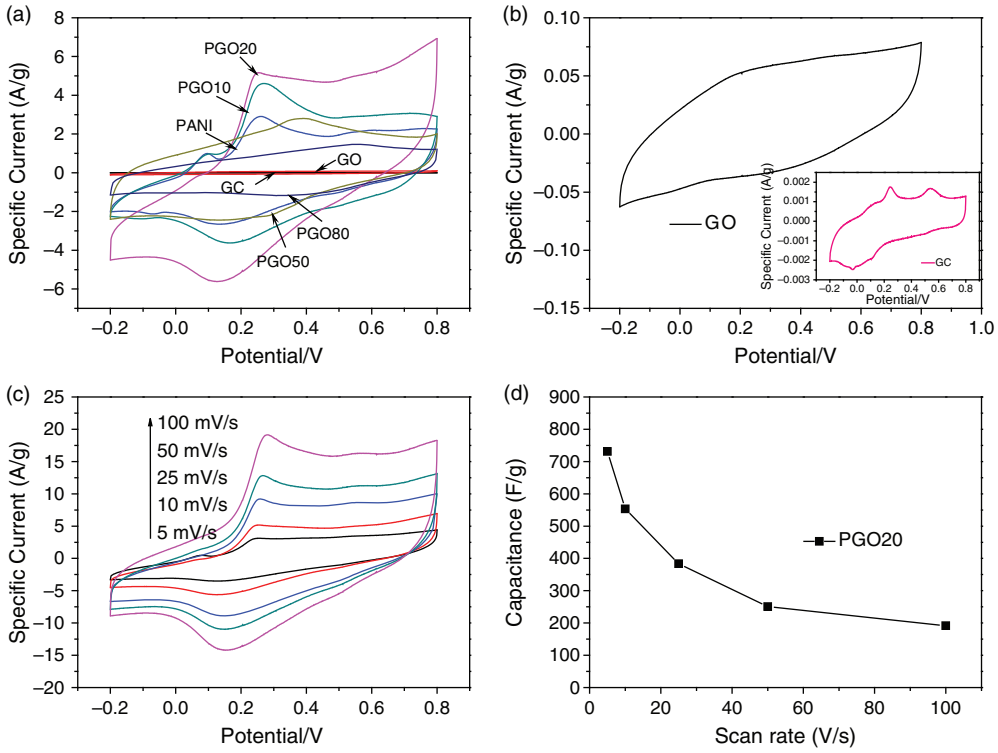

Fig. 4. Electrochemical characterization of the electrode materials: CV curves of different materials at 10 mV/s scan rate (a), CV curve of GO at the scan rate of 10 mV/s (b), and the inset is the CV curve of glassy carbon electrode at the scan rate of 10 mV/s, CV curves of PGO20 at various scan rates (c), and specific capacitance of PGO20 at various scan rates (d).

functionalities.[29] The inset of Figure 4(b) also shows that the background signal of glassy carbon is negligible. Two couples of redox peaks are observed from the CV curve of the PANI sample in Figure 4(a), corresponding to Faradic transformation of emeraldine/pernigraniline and redox transitions of leucoemeraldine form (semiconductor)/polaronic emeraldine form (conductor).[30] Similar to the reported values for the PANI based supercapacitors, a high specific capacitance of 275.8 F/g is obtained for the PANI sample. The CV forms of the PGO composites change largely with the increase of the GO/PANI mass ratios. Firstly, when the GO/PANI mass ratios change from 10% to 20%, the CV forms change little but a couple of redox peaks weakens and when that change from 50% to 80%, the forms gradually move to that of GO. This tendency may be attributed to the redox transition transformations of the PANI and the changes of electron transport paths with the increase of the GO contents in the composites. Compared with the pure PANI electrode, the specific capacitances of these composite materials firstly increase, as the GO/PANI mass ratios in composites increase, from PGO10 (399.5 F/g) to PGO20 (553.4 F/g) and decrease from PGO50 (311.3 F/g) to PGO80 (166.9 F/g). It is notable that PGO20 has the highest capacitance among these composites, which is maybe due to the synergistic interaction between the PANI hollow microspheres and the GO sheets. The GO sheets wrapped on the surface of PANI hollow microspheres not only reduce the aggregation of the PANI microspheres but also enhance their specific surface area.[31] As shown in Table I, the changes in the specific capacitances of the composites are consistent with the changes in their surface areas. Meanwhile, the GO sheets, served as the conductive channels of the electrons, strongly improve the conductivity of the composites.[8] Therefore, with the increase of the GO mass ratios in the composites, the features for PGO composites in the CV curves firstly increase due to the increase of the specific surface area and the conductive channels of the electrons, and then decrease markedly attributed to the aggregation of GO accompanied by the decline of the conductivity.

The CV curves of the PGO20 composite at different scan rates are also obtained (Fig. 4(c)). As the scan rate increases from 5 to 100 mV/s, the current responses increase significantly and the potentials of the anodic and cathodic peaks shift in more positive and negative

Table I. Summary of electrochemical properties and surface area of GO, PANI, PGO composites.

Samples	GO	PANI	PGO10	PGO20	PGO50	PGO80
Specific capacitance (F/g)	4.79	275.8	399.5	553.4	311.3	166.9
BET surface area (m^2/g)	4.32	18.49	27.26	31.05	25.83	11.33

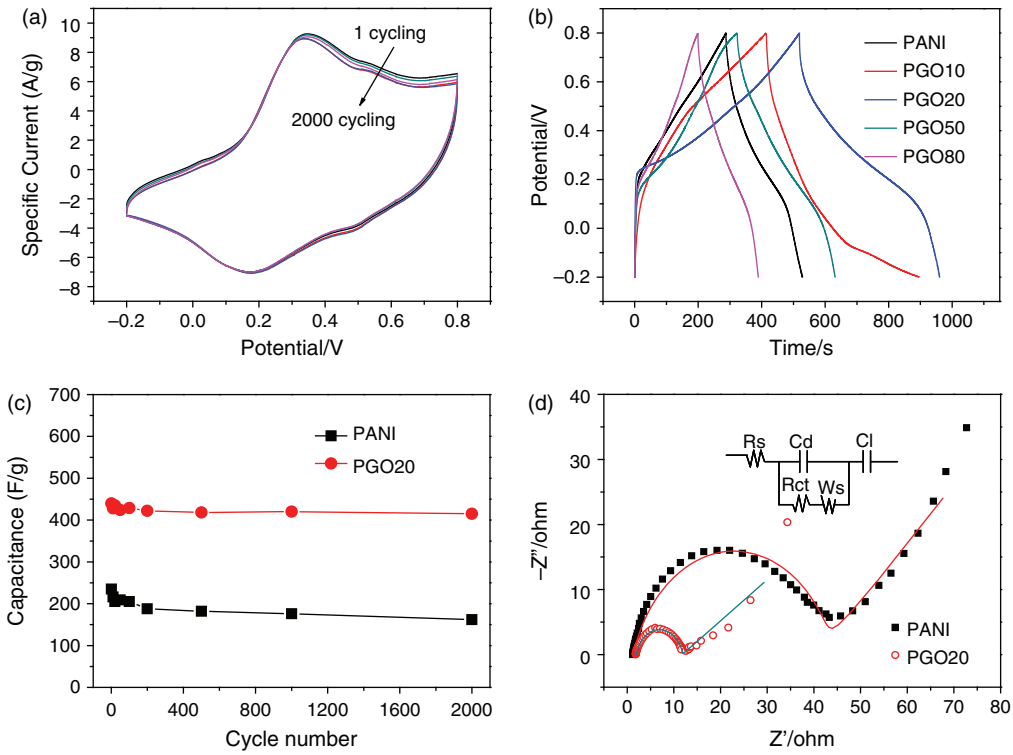

Fig. 5. Curve tests of PGO20 from 1 to 2000 cycles at the scan rate of 25 mV/s (a), charge/discharge curves of different materials at a current density of 1 A/g (b), variation in the specific capacitance of PGO20 and PANI as a function of the cycle number at a current density of 3 A/g (c), Nyquist plots (d) and the inset shows the electrical equivalent circuit of PGO20 used for fitting impedance spectra.

directions, respectively. And the features of the PGO20 composite curve at high sweeping rates are similar to those at low ones. From Figure 4(d), it is clearly seen that the specific capacitances of the PGO20 composite decrease from 731.2 F/g (5 mV/s) to 191.4 F/g (100 mV/s) with the increase in the scan rates. This behavior is due to the large electrochemical available surface resulting in high charge storage for the pseudocapacitance at low scan rate, and the slow diffusing speed of the ions in the electrolyte solution unable to satisfy the need of electrode rapid reaction.

The cycling stability of the PGO20 composite is also tested in Figure 5(a). As shown in Figure 5(a), the current response of the PGO20 composite at the scan rate of 25 mV/s remains almost constant and the peak potential position changes very little from 1 to 2000 cycles. It suggests that the introduction of the GO sheets can significantly improve the reversibility and cycling stability of the PGO composites, which are suitable for high-performance of pseduocapacitor electrodes.

To further confirm the merits of PGO composites as supercapacitor electrodes, the electrochemical properties of PANI and PGO composite electrodes are fully tested by galvanostatic charge/discharge (Fig. 5(b)) at a charging/discharging current density of 1 A/g. The shape of the curves is almost triangular, suggesting the high degree of symmetry in charge and discharge. As shown in Figure 5(b), the specific capacitances of the samples decrease in the order of PGO20 > PGO10 > PANI > PGO50 > PGO80, which is much similar to that calculated from the CV curves. The PGO20 supercapacitor has the longest charge time and the highest specific capacitance of 518.3 F/g among the samples. The specific capacitance of the PGO20 composite is much higher than these values of the amide group-connected graphene-polyaniline nanofiber hybrid[32] (361.9 F/g at 1 A/g) and the flexible graphene/polyaniline nanofiber composite[30] (205.2 F/g at 1 A/g). It is observed from Figure 5(c) that the PGO20 composites exhibit good cycling stability (95% of the preserved capacitance is conserved) than that of PANI, which is attributed to that the chemical wrapping effect promotes electrochemical stability at high current densities and exerts a synergistic effect. Therefore, the results reveal that the PGO20 composites with the high specific capacitance and cycling stability are most suitable materials for the high-performance of electrochemical pseudocapacitance.

EIS is used to examine the electrochemical conductivity behavior of the system with the frequency range from 100 kHz to 0.01 Hz. In Figure 5(d), all Nyquist plots were characterized by two distinct parts, a semi-circle at high-frequency and a linear line at low-frequency. And an equivalent circuit modeled for the impedance analysis is also shown in the inset of Figure 5(d), where two capacitors C represent double-layer capacitance (C_d) and

Table II. Fitting data for equivalent electrical circuit elements by the simulation of impedance spectra.

Samples	R_s (Ω)	R_{ct} (Ω)	W_s (S-s$^{0.5}$) × 10^{-3}	C_d (μF)	C_l (F)
PANI	1.53	43.28	0.69	324	1.25
PGO20	1.61	10.04	0.85	245	1.43

Faradic capacitance (C_l), respectively, and W_s stands for the Warburg impedance.[33] From the Nyquist plot, we can obtain the solution resistance R_s and the charge transfer resistance R_{ct} by intercepting the real Z' axis of the high-frequency semi-circle at R_s and $(R_s + R_{ct})$, respectively. From the fitting data simulated for equivalent electrical circuit elements in Table II, the two electrodes have the almost identical solution resistance values of R_s. However, the electrode of the PGO20 composite has a smaller R_{ct} (10.04 Ω) than that of the pure PANI (43.28 Ω), which implies that the PGO20 electrode has smaller charge transfer resistance. And the lower resistance and better capacitive behavior of the PGO20 electrode than that of the pure PANI electrode is mainly ascribed to the microstructure of the GO sheets wrapped on the PANI hollow microspheres. Although pure GO used as the electrode has poor electrical conductivity, the conductivity of the PGO composite (10 S cm^{-1}) largely improves than that of GO (10^{-3} S cm^{-1}) and pure PANI (2 S cm^{-1}), which can be attributed to the $\pi-\pi$ stacking between PANI and the GO sheets.[34] Sun et al.[35] also reported that the superior electrochemical property of PGO composites is due to that the GO sheets can increase electronic conductivity and reduce electrical charge transfer resistance of the PANI/GO electrode. Therefore, the synergistic effect of the PANI hollow microspheres and the GO sheets significantly improves the electrochemical performance of the composite electrode. This result is in good agreement with the capacitance values calculated from the CV curves.

4. CONCLUSIONS

In summary, we have synthesized the novel composites of PGO hollow microspheres through a facile self-assembly method for electrochemical pseudocapacitor with long cycle life. The mass ratio of PANI and GO is important to the high electrochemical performance of these composites. The PGO20 composite shows the highest specific capacitance of 731.2 F/g at a scan rate of 5 mV/s and good charge/discharge cycling stability (95% of the preserved capacitance is conserved after 2000 cycles). For practical applications, a two-electrode system will be further applied to validate the energy storage performance of the composites in the future work.

Acknowledgments: This work was supported by from the 973 project of MOST (2011CB933700), the National Natural Science Foundation of China (21071147; 91126020; 21077107), and Special Foundation for High-level Waste Disposal (2007-840). Mancheng Liu and Xilin Wu contributed equally to this paper.

References and Notes

1. P. Simon and Y. Gogotsi, *Nat. Mater.* 7, 845 **(2008)**.
2. P. J. Hall, M. Mirzaeian, S. I. Fletcher, F. B. Sillars, A. J. R. Rennie, G. O. Shitta-Bey, G. Wilson, A. Cruden, and R. Carter, *Energy Environ. Sci.* 3, 1238 **(2010)**.
3. Y. P. Zhai, Y. Q. Dou, D. Y. Zhao, P. F. Fulvio, R. T. Mayes, and S. Dai, *Adv. Mater.* 23, 4828 **(2011)**.
4. D. S. Patil, J. S. Shaikh, D. S. Dalavi, S. S. Kalagi, and P. S. Patil, *Mater. Chem. Phys.* 128, 449 **(2011)**.
5. D. Y. Liu and J. R. Reynolds, *ACS Appl. Mater. Interfaces* 2, 3586 **(2010)**.
6. G. X. Zhao, J. X. Li, L. Jiang, H. L. Dong, X. K. Wang, and W. P. Hu, *Chem. Sci.* 3, 433 **(2012)**.
7. S. B. Yang, X. L. Wu, C. L. Chen, H.L. Dong, W. P. Hu, and X. K. Wang, *Chem. Commun.* 48, 2773 **(2012)**.
8. K. Zhang, L. L. Zhang, X. S. Zhao, and J. S. Wu, *Chem. Mater.* 22, 1392 **(2010)**.
9. Q. B. Pei, G. Yu, C. Zhang, Y. Yang, and A. J. Heeger, *Science* 269, 1086 **(1995)**.
10. A. G. MacDiarmid, *Angew. Chem. Int. Ed.* 40, 2581 **(2001)**.
11. Y. Z. Long, Z. J. Chen, Y. J. Ma, Z. Zhang, A. Z. Jin, C. Z. Gu, L. J. Zhang, Z. X. Wei, and M. X. Wan, *Appl. Phys. Lett.* 84, 2205 **(2004)**.
12. K. C. Huang, C. W. Hu, C. Y. Tseng, C. Y. Liu, M. H. Yeh, H. Y. Wei, C. C. Wang, R. Vittal, C. W. Chucd, and K. C. Ho, *J. Mater. Chem.* 22, 14727 **(2012)**.
13. J. J. Xu. K. Wang, S. Z. Zu, B. H. Han, and Z. X. Wei, *ACS Nano* 4, 5019 **(2010)**.
14. L. Tan, L. J. Cao, M. Yang, G. Wang, and D. B. Sun, *Polymer* 52, 4770 **(2011)**.
15. J. G. Wang, Y. Yang, Z. H. Huang, and F. Y. Kang, *J. Power Sources* 204, 236 **(2012)**.
16. Q. Jiang, D. Y. Xie, G. G. Fu, B. Huang, X. F. Zhao, and Y. Zhao, *Mater. Sci. Forum.* 687, 61 **(2011)**.
17. N. G. Shang, P. Papakonstantinou, M. McMullan, M. Chu, A. Stamboulis, A. Potenza, S. S. Dhesi, and H. Marchetto, *Adv. Funct. Mater.* 18, 3506 **(2008)**.
18. K. S. Novoselov, A. K. Geim, S. V. Morozov, D. Jiang, Y. Zhang, S. V. Dubonos, I. V. Grigorieva, and A. A. Firsov, *Science* 306, 666. **(2004)**.
19. D. V. Kosynkin, A. L. Higginbotham, A. Sinitskii, J. R. Lomeda, A. Dimiev, K. Price, and J. M. Tour, *Nature* 458, 872 **(2009)**.
20. Z. F. Liu, Q. Liu, Y. Huang, Y. F. Ma, S. G. Yin, X. Y. Zhang, W. Sun, and Y. S. Chen, *Adv. Mater.* 20, 3924 **(2008)**.
21. Q. Liu, Z. F. Liu, X. Y. Zhang, L. Y. Yang, N. Zhang, G. L. Pan, S. G. Yin, Y. S. Chen, and J. Wei, *Adv. Funct. Mater.* 19, 894 **(2009)**.
22. Y. Liu, R. J. Deng, Z. Wang, and H. T. Liu, *J. Mater. Chem.* 22, 13619 **(2012)**.
23. H. L. Wang, J. T. Robinson, G. Diankov, and H. J. Dai, *J. Am. Chem. Soc.* 132, 3270 **(2010)**.
24. X. Guo, G. T. Fei, H. Su, and L. D. Zhang, *J. Mater. Chem.* 21, 8618 **(2011)**.
25. C. A. Amarnath, J. Kim, K. Kim, J. Choi, and D. Sohn, *Polymer* 49, 432 **(2008)**.
26. W. L. Zhang, B. J. Park, and H. J. Choi, *Chem. Commun.* 46, 5596 **(2010)**.
27. R. Cruz-Silva, J. Romero-Garcıa, J. L. Angulo-Sanchez, E. Flores-Loyola, M. H. Farıas, F. F. Castillon, and J. A. Dıaz, *Polymer* 45, 4711 **(2004)**.

ARTICLE

28. L. Q. Xu, Y. L. Liu, K. G. Neoh, E. T. Kang, and G. D. Fu, *Macromol. Rapid Commun.* 32, 684 **(2011)**.
29. Y. R. Nian and H. Teng, *J. Electrochem. Soc.* 149, A1008 **(2002)**.
30. Q. Wu, Y. X. Xu, Z. Y. Yao, A. R. Liu, and G. Q. Shi, *ACS Nano* 4, 1963 **(2010)**.
31. J. Li, H. Q. Xie, Y. Li, J. Liu, and Z. X. Li, *J. Power Sources* 196, 10775 **(2011)**.
32. J. H. Liu, J. W. An, Y. C. Zhou, Y. X. Ma, M. L. Li, M. Yu, and S. M. Li, *ACS Appl. Mater. Interfaces* 4, 2870 **(2012)**.
33. M. D. Stoller, S. J. Park, Y. W. Zhu, J. H. An, and R. S. Ruoff, *Nano Lett.* 8, 3498 **(2008)**.
34. H. L. Wang, Q. L. Hao, X. J. Yang, L. D. Lu, and X. Wang, *Electrochem. Commun.* 11, 1158 **(2009)**.
35. J. Sun and H. Bi, *Matter Lett.* 81, 48 **(2012)**.